Investigating balance control of a hopping bipedal robot

Beichen Ding[1], Andrew Plummer[1] and Pejman Iravani[1]

[1] Centre for Power Transmission and Motion Control,
Department of Mechanical Engineering,
University of Bath,
Bath, UK
b.ding@bath.ac.uk

Abstract. Legged robots are dynamic moving machines that are potentially able to traverse through rough terrain which is inaccessible for wheeled or tracked vehicles. For bipedal robots, balancing control while hopping/running is challenging, especially when the foot contact area is small. Servo hydraulics is highly suitable for robot leg actuation due to its high power density and good power-to-weight ratio. This paper presents a controller for a hydraulically actuated bipedal robot, the Bath Bipedal Hopper (BBH). The controller follows the well-established structure of the 'Three-part' control algorithm. The three parts are: hopping height control; longitudinal velocity control by changing the leg angle during the flight phase to place the foot in the desired position; and body attitude correction during the stance phase. Simulation results from a detailed non-linear model indicate that this controller can successfully balance the hydraulic robot while hopping with different longitudinal velocities.

Keywords: Bipedal hopping robot, Hydraulic actuation, Balancing controller.

1 Introduction

Legged animals are found widely in the natural world, and many are highly effective at traversing rough terrain. Similarly, legged robots present themselves with potential advantages for easily travelling through rough terrain comparing with wheeled or tracked vehicles [1]. Some successfully developed legged moving machines are summarized in [2]. The study of mono-legged or bipedal hopping robot is a sustained interest that is motivated by human`s desire to have a comprehensive understanding of this locomotion, which can also be expanded and applied to multi-legged robots. A springy leg interacting with a body mass is able to give a natural running/hopping frequency. Coil springs and compressed air are widely used to provide the required leg compliance. Servo hydraulics is highly suitable for robot leg actuation due to the high power density and quick system response. KenKen is a famous hopping robot with articulated type of leg, which takes advantage of coil spring accompanied by hydraulic actuation [3], which is shown in Fig. 1.

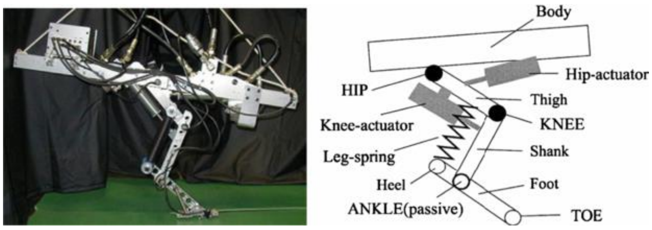

Fig. 1. Kenken: one-legged hopping robot.

Maintaining balance is an important objective for dynamic robots while walking or running. For pseudo-static multi-legged robots, balance can be achieved by keeping the body CoG above the support region created by the feet, which is called ‘Zero Moment Point’ (ZMP) control [4]. The SILO4 robot and Asimo, as shown in Fig. 2, are successfully balanced using this method while walking.

However, balancing control becomes challenging for bipedal robots when the foot contact area is small. In 1986, Raibert developed a ‘Three-part’ control algorithm to explain the basic locomotion mechanism of a one-legged case [5], for which there is only one type of gait, namely hopping. The three controlled variables are: the hopping height, the horizontal velocity and the body attitude. In order to accomplish different control actions, a distinction between the flight phase and the stance phase is necessary. During the stance phase, the one-legged robot behaves as a spring loaded inverted pendulum (SLIP) with the foot pivoted on the ground. During stance, the robot can be balanced by controlling the body rotation angle, and the leg actuator is required to accomplish the hopping height control task. During the flight phase, the horizontal velocity control can be achieved by controlling the leg angle with respect to the CoG to place the foot at required position for the next touch-down.

Several dynamic running robots were built to test this control algorithm during 1980s and 1990s, which are introduced in [6]. This controller is also extended for multi-legged robots for control the body pitching and rolling [7].

A hydraulically actuated bipedal hopping robot, called the Bath Bipedal Hopper (BBH) has been developed at the University of Bath to study motion control of legged robots. In this paper, the ‘Three-part’ control algorithm is investigated for this robot via simulation. A detailed non-linear simulation model will be developed and the controller implementation is described in the following sections.

Fig. 2. SILO4: a quadruped walking robot; Asimo: a humanoid walking robot.

2 Description of the Bath Bipedal Hopper robot

A sketch of the BBH is shown in Fig. 3. The BBH is a small-sized, hydraulically actuated bipedal hopping robot. The articulated type robot leg is composed of three links. The 1st link: a hydraulic actuator, named the leg actuator, is placed in parallel with the '*thigh*' to actuate the knee joint; the 2nd link: an extension coil spring is mounted in parallel with the '*shank*' to provide the required leg compliance; the 3rd link: a '*lower leg*' is used to connect the ankle joint and the heel joint.

The robot body is an aluminum frame for mounting the manifold, valves and PC-104 controller. A hip actuator is placed under the body to drive the hip joint. For the initial condition, the hip actuator position is controlled to give a 45° hip angle, plus the leg actuator is controlled to the mid-stroke, resulting in the body`s CoM being aligned with the foot contact point, vertically. The main dimensional specifications of the BBH are summarized in Table 1.

The test rig setup is shown in Fig. 4. A position transducer is place in parallel with each leg actuator to measure the piston position. A pressure sensor is used to measure the piston side pressure of the actuator. Additionally, an incremental encoder is added at the heel joint so that the spring displacement can be calculated using a kinematic transformation.

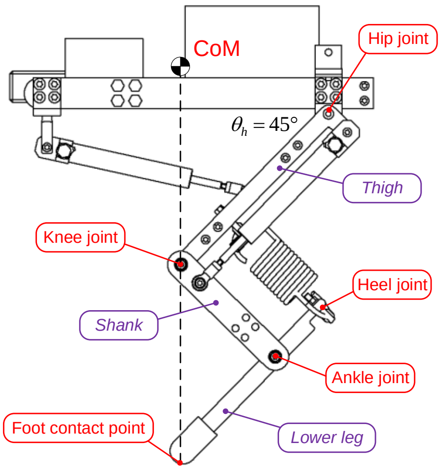

Fig. 3. Sketch of the BBH robot.

Table 1. Main dimensional specifications of the BBH robot.

Parameters	Symbol	Value	Unit
Height	*H*	552	mm
Length	*L*	400	mm
Width	*W*	315	mm
Weight	*M*	14.78	kg
Spring stiffness (physical)	*K*	9.62	N/mm

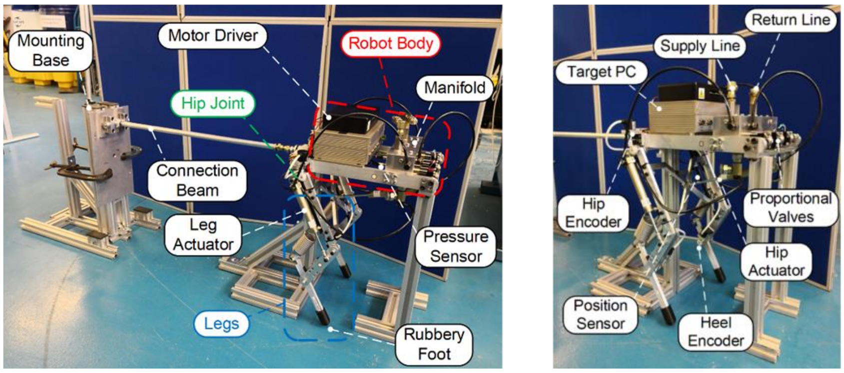

Fig. 4. The BBH robot (shown with mechanical constraint, left picture).

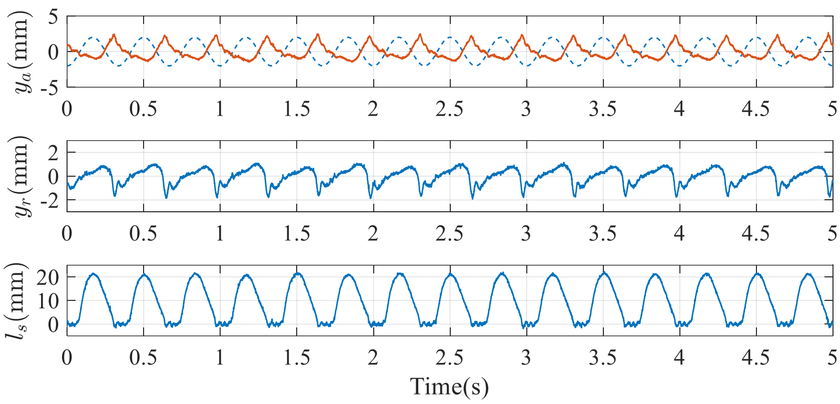

Fig. 5. Experimental results of using 3 Hz sinusoid signal to excite the leg actuator.

A primary bench test has been taken to validate the efficacy of the mechanical design of the robot. A sinusoid position signal (2 mm of the amplitude at 3Hz frequency) is used to excite the leg actuator to achieve an open loop hopping. Additionally, the two leg actuator displacements are synchronized using a 'Modal Controller'. This controls the mean of the leg actuator positions and the corresponding difference, which are called the average position (y_a) and roll position (y_r), respectively. If the demand roll position is zero, the two leg actuators are synchronized. The consistent spring displacement, l_s , in Fig. 5 indicates that the robot is hopping, plus the roll position error is mainly caused by different friction applied at each foot, left and right.

3 Modelling

3.1 Hydraulic model

The modelling follows well established procedures [8] accompanied by some findings from experiments. The hydraulic circuit is shown in Fig. 6.

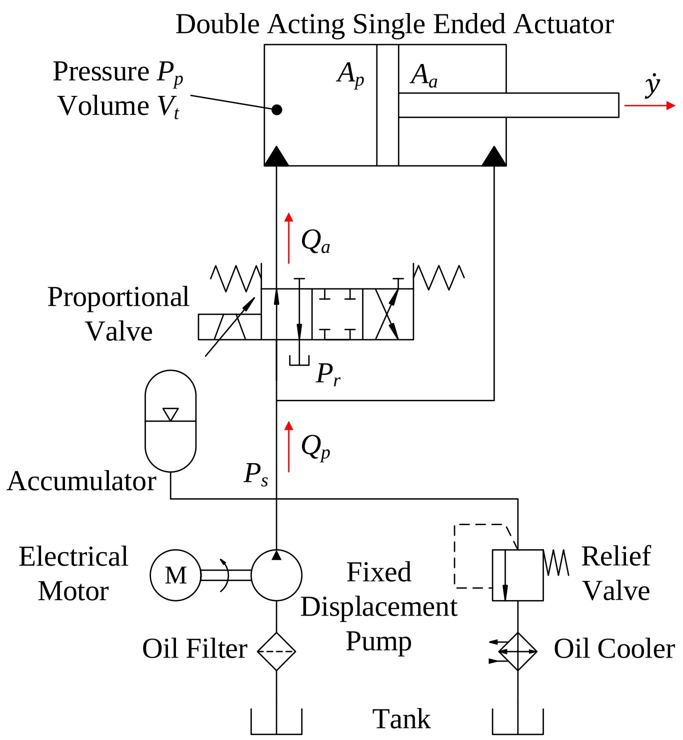

Fig. 6. Hydraulic circuit for one leg actuator.

Actuator model

Assuming there is no internal or external leakage, the hydraulic actuator is modelled by:

$$P_p A_p - P_s A_a - F_f = F_h \tag{1}$$

$$Q_a = A_p \dot{y} + \frac{V_t}{B} \dot{P}_p \tag{2}$$

where A_a is the annulus area, F_h is the actuation force, F_f is the friction, Q_a is the piston side flow rate, V_t is the trapped oil volume and B is the bulk modulus of the oil.

Additionally, the friction force is modelled by:

$$F_s = f_v \dot{y} \tag{3}$$

$$F_f = \begin{cases} F_c & \text{for } F_s \geq F_c \\ F_s & \text{for } |F_s| < F_c \\ -F_c & \text{for } F_s \leq F_c \end{cases} \tag{4}$$

where F_c is the Coulomb friction force, and F_s is velocity-dependent friction at low velocity, introduced to avoid a discontinuity which can cause numerical issues during the simulation; f_v is a friction coefficient which is relatively large.

Valve model

The proportional valve is modelled using orifice equation. Only one orifice equation is needed as the flow is only metered into one side of the actuator. The spool displacement is considered as a dimensionless variable which ranging from -1 to +1 with the closed position corresponding to 0. The valve model is given by:

$$Q_a = K_v X_v \sqrt{P_s - P_v} \tag{5}$$

where P_v is the outlet pressure, K_v is the valve flow coefficient and X_v is the normalized spool displacement. Additionally, a second-order transfer function is used to represent the valve spool dynamics, which is given by:

$$X_v = \frac{\omega_v^2}{s^2 + 2\xi_v \omega_v + \omega_v^2} \tilde{u}_c \tag{6}$$

where, $\tilde{u}_c$ is the valve driving signal, ω_v is the spool natural frequency and ξ_v is the spool damping ratio, which are empirical values determined from the manufacturer data sheet or experimental results. The hysteresis of the valve is modelled as 'backlash', as shown in Fig. 7, in which u_w is the dead-band width.

Hose pressure loss model.

The model of the pressure loss between the valve and the cylinder is given by:

$$Q_a = K_h \sqrt{P_p - P_v} \tag{7}$$

where K_h is the hose pressure loss factor, which is an empirical value.

The parameter values of the hydraulic models are provided in Table 2.

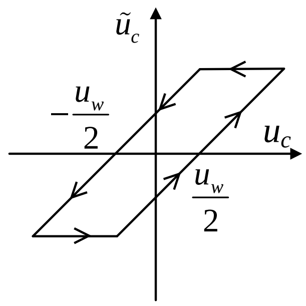

Fig. 7. Valve hysteresis.

Table 2. Parameter values of the hydraulic models.

Parameters	Symbol	Value	Unit
Supply pressure	P_s	160×10^5	Pa
Return pressure	P_r	0	Pa
Piston area	A_p	1.13×10^{-4}	m^2
Annulus area	A_a	0.63×10^{-4}	m^2
Valve flow coefficient	K_v	4.89×10^{-8}	$m^4/s/N^{1/2}$
Valve spool natural frequency	ω_v	942.48	rad/s
Valve spool damping ratio	ξ_v	0.7	
Backlash deadband width	u_w	0.2	A
Coulomb friction (actuator piston)	F_f	105	N

3.2 Mechanical model

The mechanical model of the BBH, which effectively is a planar robot, is built using SimMechanics®, a multi-body mechanical simulation tool in Simulink®. The mechanical properties of the rigid bodies are defined in Autodesk Inventor 2017®, then uploaded to SimMechanics® to create a 3D visualization.

A 'spring and damper force' block is used to represent the spring force between the connections on upper leg and lower leg. Modelling the ground contact is an important issue. The reaction force from the ground should support the robot vertically (y-axis) and prevent horizontal foot slip (z-axis) during the stance phase. Define the coordinate of the robot foot contact point is $(0, y_n, z_t)$ and the corresponding projection to the ground is $(0, y_n', z_t')$. The ground reaction force is modelled as a spring and damper both vertically and horizontally. The ground stiffness is relatively large so as not to significantly reduce the effective robot leg`s stiffness. Thus, the vertical reaction force and the horizontal friction force are given by:

$$F_y = \begin{cases} -k_y\left(y_n - y_n'\right) - b_y\left(\dot{y}_n - \dot{y}_n'\right) & \text{for stance phase} \\ 0 & \text{for flight phase} \end{cases} \tag{8}$$

$$F_z = \begin{cases} -k_z\left(z_t - z_t'\right) - b_z\left(\dot{z}_t - \dot{z}_t\right) & \text{for stance phase} \\ 0 & \text{for flight phase} \end{cases} \tag{9}$$

where F_y is the vertical reaction force, k_y is the ground normal spring stiffness and b_y is the ground normal damping coefficient. F_z is the horizontal friction force, k_z is the tangential spring stiffness and b_z is the tangential damping coefficient. Combining with the hydraulic models implemented in Simulink®, the top level of the simulation model and the 3D visualization is shown in Fig. 8. Numerical implementation is performed by a stiff/Mod. Rosenbrock solver (Simulink`s ODE23s) with variable step size, which is a compromise between the computing speed and the simulation accuracy.

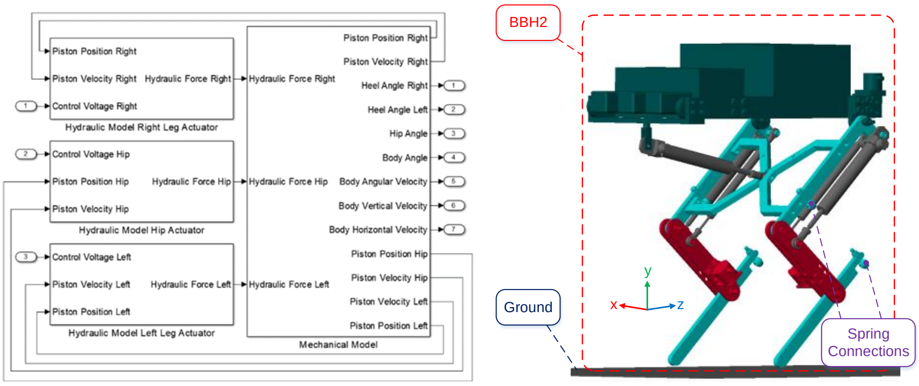

Fig. 8. Top level of the simulation model and 3D visualization.

4 Controller implementation

To simplify the controller implementation, the distance between the body CoG and the foot is introduced as a '*virtual leg*'. The leg displacement is calculated using a kinematics transformation. Fig. 9 is a simplified diagram of one hopping cycle.

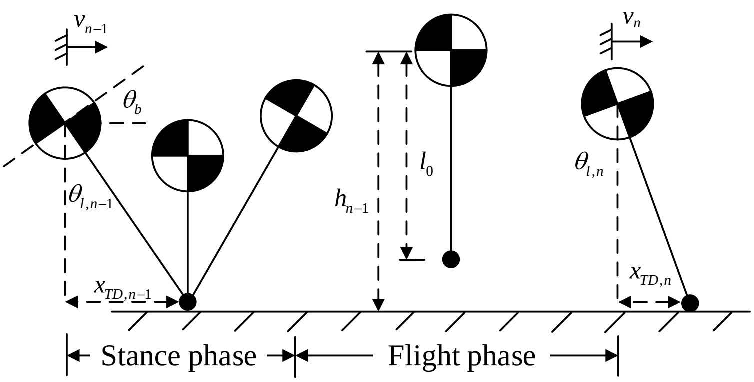

Fig. 9. Simplified diagram of one hopping cycle.

4.1 Control of the hopping height

Bhatti et al developed a simple hopping height control technique for a planar robot travelling over discontinuous surfaces in [9]. The leg actuator demand velocity during the stance phase is derived using the achieved height of the previous hop, denoted $h_{n-1,a}$, and the desired height for the next hop, $h_{n,d}$, and is given by:

$$q_{n,d} = K_{h1}\sqrt{h_{n,d}} + K_{h2}\left(\sqrt{h_{n,d}} - \sqrt{h_{n-1,a}}\right) \tag{10}$$

where $q_{n,d}$ is the desired extension velocity of the leg, K_{h1} and K_{h2} are the controller gains. Integrating this desired velocity gives the demand position, which is common for servo-hydraulics system. Additionally, the virtual leg is controlled to return to mid-length during the flight phase to be ready for the next touch-down, plus the demand hopping height remains constant in this simulation, i.e. $h_{n,d} = 0.43\,\mathrm{m}$. The closed-loop leg length control is achieved using a PI controller:

$$u_c = K_p e + K_i \int e dt \tag{11}$$

where K_p is the proportional gain, K_i is the integral gain and e is the leg position error.

4.2 Control of the longitudinal velocity

During the flight phase, the robot has a parabolic trajectory, thus moving the hip actuator results in different rotation angle for the body and legs due to the moment of inertia. The leg angle, θ_l , is controlled to place the foot on the ground at horizontal position, x_{TD} , relative to the body CoG, to achieve the required longitudinal velocity.

An appropriate leg angle for the next touch-down can be calculated from the previous hop. Thus, the foot placement at the previous touch-down, $x_{TD,n-1,a}$, is given by:

$$x_{TD,n-1,a} = \frac{1}{2} v_{n-1,a} T_{s,n-1,a} \tag{12}$$

where $v_{n-1,a}$ is the achieved body longitudinal velocity at previous touch-down and $T_{s,n-1,a}$ is the corresponding stance duration.

Thus the leg angle is given by:

$$\theta_{l,n-1,a} = \sin^{-1} \frac{x_{n-1,TD,a}}{l_0} \tag{13}$$

where $\theta_{l,n-1,a}$ is the achieved leg angle of the previous hop and l_0 is the nominal length of the virtual leg, which is 0.4 m.

According to small perturbation approximation, define:

$$\Delta\theta_l = K_l \left(v_{n,d} - v_{n-1,a} \right) \tag{14}$$

where $v_{n,d}$ is the desired body longitudinal velocity for the next touch-down, $\Delta\theta_l$ is the corresponding leg angle change and K_l is the feedback gain. Thus, the desired leg angle for the next touch-down, $\theta_{l,n,d}$, is given by:

$$\theta_{l,n,d} = \theta_{l,n-1} + \Delta\theta_l \tag{15}$$

If hip torque is the control variable, leg angle can be controlled in closed loop, thus:

$$\tau_l = K_{l1}\left(\theta_{l,n} - \theta_{l,n,d}\right) + K_{l2}\left(\dot{\theta}_{l,n}\right) \tag{16}$$

where τ_l is the control torque for the hip during flight phase, K_{l1} and K_{l2} are feedback gains, and $\theta_{l,n}$ is the actual leg angle.

4.3 Control of the body attitude

Controlling the leg angle during flight phase changes the body pitch angle, which can be corrected during the stance phase. It is assumed there is a sufficient friction at the ground to avoid the robot foot slipping. The body angle, θ_b, is controlled towards a horizontal position, i.e. $\theta_{b,d} = 0^\circ$, using a simple servo given by:

$$\tau_b = K_{b1}\left(\theta_b - \theta_{b,d}\right) + K_{b2}\left(\dot{\theta}_b\right) \tag{17}$$

where τ_b is the control torque for the hip during stance phase, K_{b1} and K_{b2} are feedback gains, and $\theta_{b,d}$ is the desired body angle.
Table 3 shows the values of the controller gains and feedback gains used in this simulation.

Table 3. Controller and feedback gains.

Parameters	Value	Unit
K_{h1}	0.02	$m^{1/2}/s$
K_{h2}	1	$m^{1/2}/s$
K_{l1}	100	Nm/rad
K_{l2}	0.02	Nms/rad
K_{b1}	1×10^5	Nm/rad
K_{b2}	9×10^3	Nms/rad
K_p	320	1/m
K_i	100	1/(sm)

5 Simulation results

Fig. 10. shows the simulation results. The simulation starts with a free drop of the robot from a small initial body height. Note that y is the actual body height. The achieved hopping frequency is approximately 3 Hz and the hopping height controller is able to correct the robot motion within several hops when the longitudinal velocity, $\dot{x}$, is changing. The leg angle is adjusted by the controller to achieve different velocity demands. At $t = 6$, a sudden movement of the hip actuator is found due to a large step change of the velocity demand, so more hops are needed to allow the robot to gradually achieve the demand velocity. Between $t = 5$ and 10, the forward traveling

speed is 0.24 m/s; between $t = 15$ and 20, the backward speed is 0.08 m/s; between $t = 20$ and 25, the backward speed is 0.15 m/s. The body angle is successfully controlled to maintain balance, not only when hopping on a spot, i.e. $\dot{x}(t) = 0$, but also to be balanced with different moving speed. The hip angle, θ_h, keeps adjusting associate with body balancing.

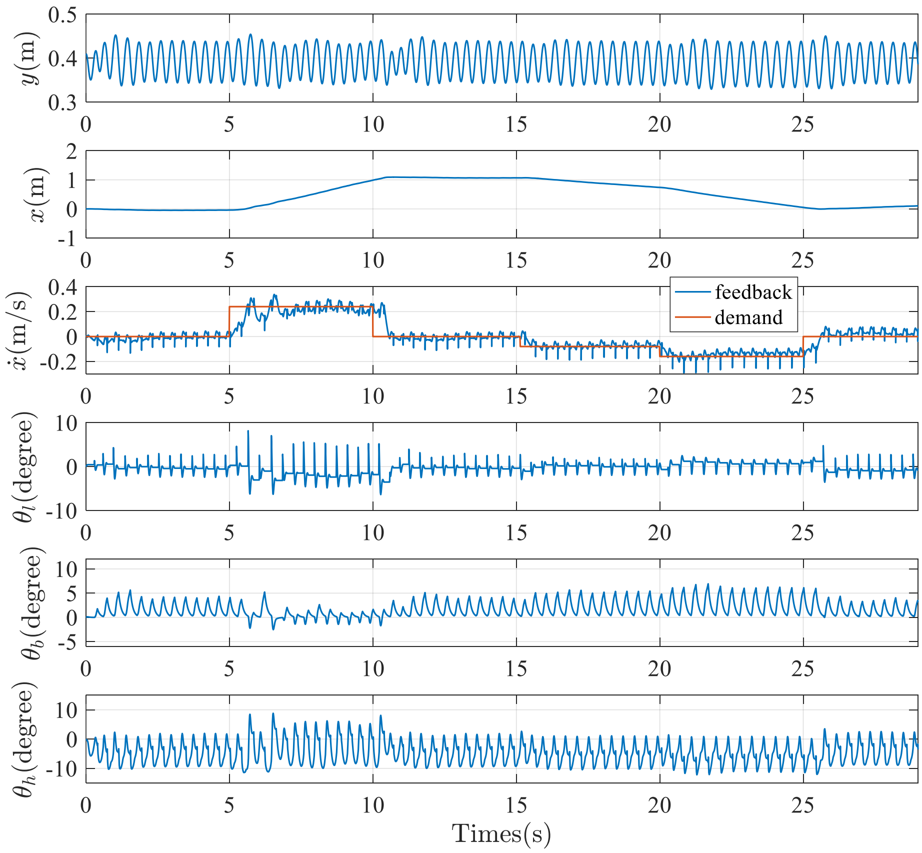

Fig. 10. Simulation results.

6 Conclusion

The investigation of the control of a bipedal robot while hopping is under taken in this paper. The bench test results indicate the efficacy of the mechanical design of the BBH robot. A detailed non-linear simulation model accompanied by physical empirical data is developed. The implemented controller is built according to the well-established 'Three-part' control algorithm. The hopping height is controlled using an adaptive controller; changing the leg angle during the flight phase to place the foot in the desired position is able to achieve longitudinal velocity control; the body attitude is controlled during the stance phase to maintain balance. The simulation results demonstrate that the controller can successfully balance the robot while hopping with different longitudinal velocities, e.g. traveling forward at 0.24 m/s, backward at 0.08 m/s or 0.15 m/s.

The practical implementation of this controller is challenging, mainly due to the performance of the sensors and signal processing, e.g. the direct measurement of the robot hopping height and longitudinal velocity requires sufficiently quick response and high measurement accuracy of the sensors. If necessary, state estimators or observers can be built, i.e. derive the hopping height or longitudinal velocity from the estimated state variables.

References

1. Sayyad, A., Seth, B., Seshu, P.: Single-legged hopping robotics research—A review. Robotica, 25(5), pp.587-613 (2007).
2. Bhatti, J., Plummer, A.R., Iravani, P., Ding, B.: A survey of dynamic robot legged locomotion. In: Fluid Power and Mechatronics (FPM), 2015 International Conference on IEEE, pp. 770-775, July 2015.
3. Hyon, S.H., Mita, T.: Development of a biologically inspired hopping robot-" Kenken". In: Robotics and Automation, 2002. Proceedings. ICRA'02. IEEE International Conference on IEEE, Vol. 4, pp. 3984-3991, May 2002.
4. Al-Shuka, H.F., Corves, B., Zhu, W.H., Vanderborght, B.: Multi-level control of zero-moment point-based humanoid biped robots: a review. Robotica, 34(11), pp.2440-2466, (2016).
5. Raibert, M.H.: Hopping in legged systems—modeling and simulation for the two-dimensional one-legged case. IEEE Transactions on Systems, Man, and Cybernetics, (3), pp.451-463, (1984).
6. MIT Leg Laboratory. http://www.ai.mit.edu/projects/leglab/
7. Raibert, M., Chepponis, M., Brown, H.B.J.R.: Running on four legs as though they were one. IEEE Journal on Robotics and Automation, 2(2), pp.70-82, (1986).
8. Plummer, A.R.: A detailed dynamic model of a six-axis shaking table. Journal of earthquake engineering, 12(4), pp.631-662, (2008).
9. Bhatti, J., Plummer, A.R., Sahinkaya, M.N., Iravani, P., Guglielmino, E., Caldwell, D.G.: Fast and adaptive hopping height control of single-legged robot. In: the11th Biennial Conference on Engineering Systems Design and Analysis. American Society of Mechanical Engineers, pp. 303-309, July 2012.